Hole- and Electron-Vibrational Couplings in Oligoacene Crystals: Intramolecular Contributions

V. Coropceanu, M. Malagoli, D. A. da Silva Filho, N. E. Gruhn, T. G. Bill, and J. L. Brédas
Department of Chemistry, The University of Arizona, Tucson, Arizona, 85721-0041
(Received 7 June 2002; published 20 December 2002)

The hole-vibrational coupling is reported for anthracene, tetracene, and pentacene on the basis of a joint experimental and theoretical study of ionization spectra using high-resolution gas-phase photoelectron spectroscopy and first-principles correlated quantum-mechanical calculations. The hole-vibrational coupling is found to be significantly smaller than the electron-vibrational coupling in the case of these oligomers; however, both quantities are predicted to converge to the same value when increasing the chain length.

DOI: 10.1103/PhysRevLett.89.275503 PACS numbers: 63.20.Kr, 31.15.Ar, 33.60.Cv

Molecular organic semiconductors in general and oligoacenes, in particular, are currently the object of much interest because of their potential applications in (opto)electronic devices [1,2]. Understanding the charge transport mechanism of these materials is a key point for device design and performance.

The experimental data point towards the necessity of applying polaronic concepts in order to rationalize the electrical properties of organic semiconductors [3,4]. The observed crossover from coherent bandlike charge transport at low temperatures to incoherent hopping motion at high temperatures [3,5] is in line with general predictions of the small polaron theory [6–8]. The electron-phonon mechanism has also been invoked to explain the electric field dependence of the charge-carrier mobilities [3,9]. Interactions with both inter- and intramolecular vibrations, which act separately or simultaneously, have been considered in the construction of polaron models. However, a detailed knowledge of the carrier-phonon coupling constants, needed for the complete understanding of the charge transport in oligoacenes, is still lacking.

In the case of organic molecular crystals with weak van der Waals intermolecular interactions, the contribution of intramolecular vibrations to the dimensionless carrier-phonon coupling constant can be estimated from [10]:

$$\lambda_{\text{e-v}} = N(E_F) \sum_i \frac{1}{4\pi^2 M_i \nu_i^2} \left(\frac{\partial h_{kk}}{\partial Q_i} \right)^2. \quad (1)$$

Here, $N(E_F)$ is the density of states at the Fermi level (per molecule and per spin) that is determined by the *intermolecular* electronic coupling between π levels [10]. The second term represents a summation over *intramolecular* vibrations; ν_i and M_i are the frequency and the reduced mass of the vibrational mode Q_i, respectively; $\partial h_{kk}/\partial Q_i$ is the diagonal vibronic matrix element for the electron (hole) state k, which can be approximated as the lowest unoccupied molecular orbital (highest occupied molecular orbital).

At the microscopic level, the charge transport mechanism can be described as a self-exchange electron transfer process from a charged oligomer to an adjacent neutral oligomer. In the context of electron transfer theory, the second term in Eq. (1) represents Marcus intramolecular reorganization energy λ_{reorg} [11]. The reorganization energy essentially corresponds to the sum of the geometry relaxation energies when going from the neutral-state geometry to the charged-state geometry ($\lambda_{\text{rel}}^{(1)}$) and vice-versa ($\lambda_{\text{rel}}^{(2)}$) [4]. These two contributions to λ_{reorg} are typically nearly identical [12]. Thus, λ_{reorg} is a measure of the strength of the hole-phonon or electron-phonon interaction and provides a direct link between the geometric and electronic structure and the transport properties of the material.

In this Letter, we discuss the strength of the hole-phonon interaction in anthracene, tetracene, and pentacene on the basis of a joint experimental and theoretical study of the fine structure of the ionization spectrum. We have carried out high-resolution gas-phase ultraviolet photoelectron spectroscopy (UPS) measurements and performed first-principles correlated quantum-mechanical calculations at the density functional theory (DFT) level [13].

The relaxation energy λ_{rel} of an isolated molecule (with $\lambda_{\text{rel}} \approx \lambda_{\text{reorg}}/2$) can be determined by analysis of its gas-phase UPS spectrum [14]. The vibrational structure present in an ionization band can be analyzed to provide the values of the Huang-Rhys factors, S, which in the framework of the harmonic oscillator model are related to λ_{rel} by:

$$\lambda_{\text{rel}} = \sum S_k h \nu_k, \quad (2)$$

where h is Planck's constant.

The He I gas-phase UPS spectra were recorded on an instrument built around a 36 cm radius hemispherical analyzer (McPherson, 10 cm gap) with photon sources, counter interface, and collection methods that have been described elsewhere [15]. The argon $^2P_{3/2}$ ionization at

15.759 eV was used as an internal calibration lock of the energy, and the $CH_3I\ ^2E_{1/2}$ ionization at 9.538 eV provided an external calibration of the energy scale. The instrument resolution (measured as the FWHM of the argon $^2P_{3/2}$ ionization) was 0.018–0.028 eV during data collection. The sample cell temperature was monitored with a *K*-type thermocouple passed through a vacuum feed through and attached directly to the ionization cell. The pentacene sample was provided by Kahn (Princeton) and used with no additional purification. Samples of anthracene (99 + %) and tetracene (98%) were purchased from Aldrich and used as received. There was no evidence of decomposition or contamination either in the gas phase or as a solid residue for any of the samples. The data were collected at 100 ± 10 °C for anthracene, 180 ± 10 °C for tetracene, and 235 ± 5 °C for pentacene. The spectra are intensity corrected according to the analyzer intensity function.

The gas-phase photoelectron spectra of anthracene, tetracene, and pentacene are shown in Fig. 1. The spectra are, in general, similar to those previously reported [16,17] although the reported first ionization energies can differ from those measured here by up to 0.2 eV.

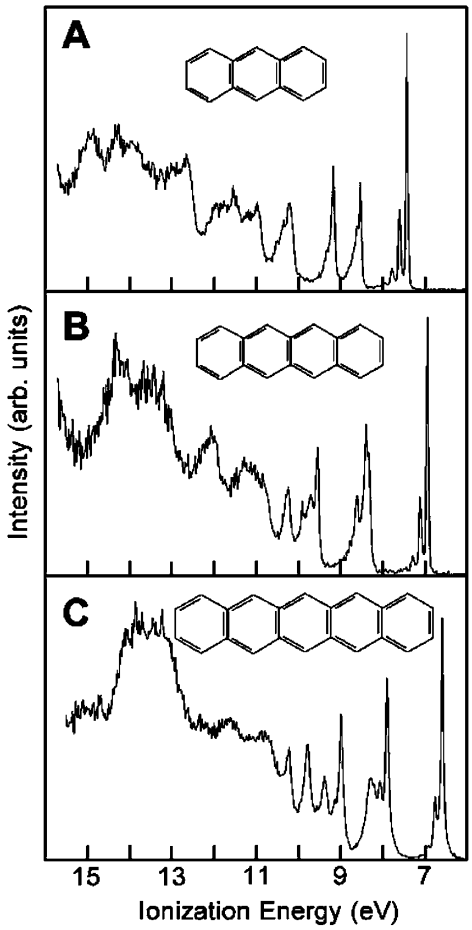

FIG. 1. Gas-phase He I UPS spectra of anthracene (A), tetracene (B), and pentacene (C).

The first ionizations are measured to have vertical energies of 7.421 eV for anthracene, 6.939 eV for tetracene, and 6.589 eV for pentacene (all vertical ionization energies are ±0.001 eV). For each molecule, several ionizations, including the first ionization, contain partially resolved vibrational fine structure. Closeups of the first ionizations that show this structure in more detail are given in Fig. 2. The data shown in this figure have been deconvoluted using a series of asymmetric Gaussians to allow a quantitative analysis of the vibrational structures [18]; the information coming from these fits is given in Table I.

The first ionization of each molecule clearly exhibits a high-frequency progression of about 0.17 eV ($\approx$1400 cm^{-1}) which lies in the region expected for C–C stretching modes. The intensities of this progression resembles a Poisson distribution:

$$I_n = \frac{S^n}{n!} e^{-S}, \tag{3}$$

where I_n is the intensity of the *n*th vibrational band. There

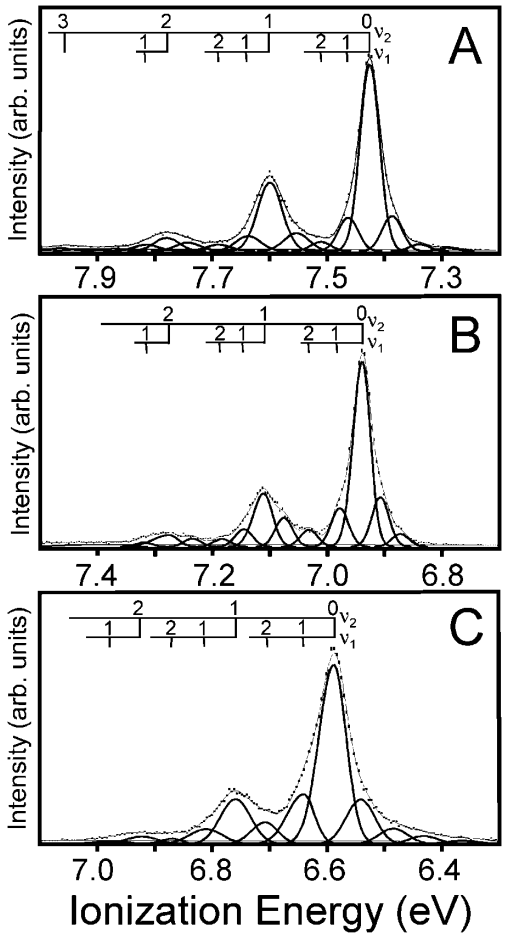

FIG. 2. High resolution closeups of the first ionizations of anthracene (A), tetracene (B), and pentacene (C). The Gaussians used for the deconvolution are shown with a thick solid line. The thin solid lines represent the overall fit, while the dots correspond to the experimental data.

TABLE I. Vibrational energies, ν (meV), Huang-Rhys factors, S, and relaxation energies, λ_{rel} (meV), obtained from the analysis of the UPS spectra of anthracene, tetracene, and pentacene. The λ_{rel} values between parentheses for pentacene are explained in the text.

	Anthracene			Tetracene			Pentacene		
	ν (meV)	S	λ_{rel} (meV)	ν (meV)	S	λ_{rel} (meV)	ν (meV)	S	λ_{rel} (meV)
Mode 1	42.3	0.182	7.7	40.9	0.184	7.6	59.9	0.279	16.7 (7.7)
Mode 2	173.3	0.358	62.0	174.1	0.294	51.2	167.1	0.251	41.9
Total			69.7			58.8			58.6 (49.6)

is also a contribution from one or more lower frequency vibrations. The spectral fits shown in Fig. 2 with the numerical values given in Table I were performed using one additional lower frequency vibrational mode to model the additional vibrational structure and hot bands of the first ionizations [19]. For all three molecules, the largest contribution to λ_{rel} is from the higher energy vibrational frequency. The contribution of the second mode is equal for anthracene and tetracene and accounts for about 11%–13% of the total intensity; in pentacene, this contribution rises up to 30%. However, in the case of pentacene, the fit to the harmonic model for the lower frequency is not as good as for the high-frequency progression; this suggests that other contributions, for instance, from nonadiabatic interactions, are also present. Therefore, the reorganization energy for pentacene has been corrected (values given in parentheses in Table I) by assuming the same contribution for the lower frequency mode as in anthracene and tetracene (the corrected values for pentacene will be used in the remainder of this work as they provide very consistent results).

The quantum-mechanical geometry optimizations have been performed at the DFT-B3LYP level using the 6-31G** basis sets. The bond-length modifications on going from the neutral to the electron- and hole-doped oligomers show a consistent trend along the series. Anthracene shows the largest geometry relaxations, with changes in C–C bond lengths on the order of 0.020 Å. This value is reduced to 0.015 and 0.010 Å in tetracene and pentacene, respectively. The geometry distortions, as well as the changes in Mulliken population, are sizeable over the whole oligomers, indicating that even for the larger oligomer, pentacene, the molecular size is still smaller than the molecular polaron extension. The theoretical estimates of the relaxation energies of the cation state and of the neutral state as obtained from the calculations of the adiabatic potential surfaces are collected in Table II. A second estimate, which provides as well the partition of the total relaxation (reorganization) energy into the contributions from each vibrational mode, has been obtained on the basis of a normal-mode analysis:

$$\lambda_{rel} = \sum 2\pi^2 \nu_i^2 M_i (\Delta Q_i)^2. \quad (4)$$

Here, ΔQ_i is the change in normal coordinate between the neutral and ionized molecules. As seen from Table II, the results obtained from both methods are in excellent mutual agreement. The normal-mode calculations further confirm the experimental finding that a major contribution to the reorganization energy is provided by high-frequency modes. In the case of anthracene, for instance, five modes in the range 150–200 meV account for 99% of the total relaxation energy.

We now turn to an estimate of the dimensionless hole-vibrational coupling $\lambda_{h\text{-}v}$. Assuming the same density of states at the Fermi level for the three systems, estimated as $N(E_F) \approx 2\ (\text{eV})^{-1}$ [10], and taking the reorganization energy as twice the experimental value of λ_{rel}, Eq. (1) yields values of 0.279, 0.235, and 0.198 for $\lambda_{h\text{-}v}$ in anthracene, tetracene, and pentacene crystals, respectively. Figure 3 shows that the hole-vibrational coupling, as predicted in Ref. [10], is inversely proportional to the number of atoms along the π-conjugated backbone.

In Table II, we also present the estimates of electron-vibrational couplings considering an electron transfer process from a radical anion to a neutral molecule. As for the hole-phonon coupling, both DFT methods, B3LYP(AP) and B3LYP(NM), provide similar results that are in very good agreement with previous calculations [10,20]. It is important to note, however, that in this

TABLE II. Theoretical estimates of relaxation energies, λ_{rel} (meV), and reorganization energies, λ_{reorg} (meV), related to the hole- and electron-vibrational couplings for anthracene, tetracene, and pentacene.

	Anthracene			Tetracene			Pentacene		
	$\lambda_{rel}^{(1)}$	$\lambda_{rel}^{(2)}$	λ_{reorg}	$\lambda_{rel}^{(1)}$	$\lambda_{rel}^{(2)}$	λ_{reorg}	$\lambda_{rel}^{(1)}$	$\lambda_{rel}^{(2)}$	λ_{reorg}
Hole									
B3LYP (AP)[a]	68	69	137	56	57	113	48	49	97
B3LYP (NM)[b]	66	70	136	57	56	113	51	49	100
Electron									
B3LYP (AP)[a]	100	96	196	81	79	160	66	66	132
B3LYP (NM)[b]	102	100	202	77	80	157	60	65	125
LDA[c]			166			130			
B3LYP[d]			186			154			127

[a]This work. Values computed from analysis of the adiabatic potential (AP) surfaces of the neutral and charged states [12].
[b]This work. Values computed from normal-mode (NM) calculations.
[c]Obtained in Ref. [10] by computing vibronic and force constants at the local density approximation level.
[d]B3LYP estimates from Ref. [20] using the same approach as in Ref. [10].

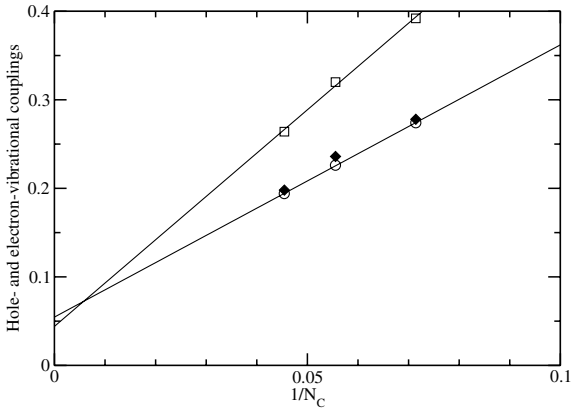

FIG. 3. Hole-vibrational coupling [◆-Exp, ○-B3LYP(AP)] and electron-vibrational coupling [□-B3LYP(AP)] vs the inverse of the number of carbon atoms in anthracene, tetracene, and pentacene.

case, in addition to high-frequency modes, there is as well a strong interaction with a low-frequency mode around 30–50 meV. Assuming the same $N(E_F)$ as in the case of hole transport, the calculations based on normal-mode analysis yield 0.404, 0.314, and 0.250 for the dimensionless electron-vibrational parameter $\lambda_{e\text{-}v}$ in anthracene, tetracene, and pentacene, respectively. As seen from Fig. 3, the electron-vibrational and hole-vibrational couplings exhibit similar trends as a function of conjugation length. However, the electron-vibrational coupling is significantly stronger than the hole-vibrational coupling for the smaller oligomers and evolves more sharply from one molecule to the next. In the limit of infinite conjugation length, both quantities converge to the same limiting value around 0.05.

To summarize, we have obtained an experimental estimate of the strength of the interaction between holes and intramolecular vibrations in anthracene, tetracene, and pentacene. Our results suggest that this interaction is significant and should be considered for the understanding of the general picture of charge transport in oligoacene systems. In particular, the interactions with intramolecular modes might be partially responsible for the observed high-field effects such as velocity saturation. The coupling with intramolecular vibration could also be important in rationalizing the difference in temperature dependence of hole and electron mobilities due to the fact that only electrons interact with low-frequency intramolecular vibrations.

This work was partly supported by NSF (CHE-0078819), ONR, PRF, and the IBM Shared University Research program.

[1] C. W. Tang and S. A. VanSlyke, Appl. Phys. Lett. **51**, 913 (1987).
[2] S. F. Nelson *et al.*, Appl. Phys. Lett. **72**, 1854 (1998).
[3] M. Pope and C. E. Swenberg, *Electronic Processes in Organic Crystals and Polymers* (Oxford University, New York, 1999), 2nd ed.
[4] E. A. Silinsh *et al.*, Chem. Phys. **198**, 311 (1995).
[5] L. B. Schein *et al.*, Phys. Rev. Lett. **40**, 197 (1978).
[6] T. Holstein, Ann. Phys. (N.Y.) **8**, 343 (1959).
[7] M. W. Wu and E. M. Conwell, Chem. Phys. Lett. **266**, 363 (1997).
[8] V. M. Kenkre *et al.*, Phys. Rev. Lett. **62**, 1165 (1989).
[9] W. Warta and N. Karl, Phys. Rev. B **32**, 1172 (1985).
[10] A. Devos and M. Lannoo, Phys. Rev. B **58**, 8236 (1998).
[11] R. A. Marcus, Rev. Mod. Phys. **65**, 599 (1993).
[12] M. Malagoli and J. L. Brédas, Chem. Phys. Lett. **327**, 13 (2000).
[13] M. J. Frisch *et al.*, *Gaussian 98 (Revision A.7)* (Gaussian, Inc., Pittsburgh, 1998).
[14] G. L. Closs and J. R. Miller, Science **240**, 440 (1988).
[15] J. Cornil *et al.*, J. Phys. Chem. A **105**, 5206 (2001).
[16] P. A. Clark *et al.*, Helv. Chim. Acta **55**, 1415 (1972).
[17] R. Boschi *et al.*, Faraday Discuss. Chem. Soc. **54**, 116 (1972).
[18] D. L. Lichtenberger and A. S. Copenhaver, J. Electron Spectrosc. Relat. Phenom. **50**, 335 (1990).
[19] N. E. Gruhn *et al.*, J. Am. Chem. Soc. **124**, 7918 (2002).
[20] T. Kato *et al.*, J. Chem. Phys. **116**, 3420 (2002).